Molecular Biology of the Cell
Vol. 14, 1002–1016, March 2003

Specification of Actin Filament Function and Molecular Composition by Tropomyosin Isoforms

Nicole S. Bryce,* Galina Schevzov,* Vicki Ferguson,* Justin M. Percival,* Jim J.-C. Lin,† Fumio Matsumura,‡, James R. Bamburg,§ Peter L. Jeffrey,¶ Edna C. Hardeman,‖ Peter Gunning,* and Ron P. Weinberger*#@

*Oncology Research Unit, Department of Paediatrics and Child Health, University of Sydney, The Children's Hospital at Westmead, Westmead NSW 2145, Australia; †Department of Biological Sciences, The University of Iowa, Iowa City, Iowa; ‡Department of Molecular Biology and Biochemistry, Rutgers University, Nelson Labs, Busch Campus, Piscataway, New Jersey; §Department of Biochemistry and Molecular Biology, Colorado State University, Fort Collins, Colorado; and ¶Developmental Neurobiology and ‖Muscle Development Units, Children's Medical Research Institute, Westmead, NSW 2145, Australia

Submitted April 30, 2002; Revised October 28, 2002; Accepted November 22, 2002
Monitoring Editor: Thomas D. Pollard

The specific functions of greater than 40 vertebrate nonmuscle tropomyosins (Tms) are poorly understood. In this article we have tested the ability of two Tm isoforms, TmBr3 and the human homologue of Tm5 ($hTM5_{NM1}$), to regulate actin filament function. We found that these Tms can differentially alter actin filament organization, cell size, and shape. $hTm5_{NM1}$ was able to recruit myosin II into stress fibers, which resulted in decreased lamellipodia and cellular migration. In contrast, TmBr3 transfection induced lamellipodial formation, increased cellular migration, and reduced stress fibers. Based on coimmunoprecipitation and colocalization studies, TmBr3 appeared to be associated with actin-depolymerizing factor/cofilin (ADF)-bound actin filaments. Additionally, the Tms can specifically regulate the incorporation of other Tms into actin filaments, suggesting that selective dimerization may also be involved in the control of actin filament organization. We conclude that Tm isoforms can be used to specify the functional properties and molecular composition of actin filaments and that spatial segregation of isoforms may lead to localized specialization of actin filament function.

INTRODUCTION

The actin microfilament network is a primary cytoskeletal system involved in the development and maintenance of morphology within cells. The dynamic nature of the actin-based system and its organization is thought to regulate specific structural changes within different cellular regions (Gunning *et al.*, 1998b). The function and form of the actin cytoskeleton is largely determined by actin-binding proteins that are associated with the polymeric structure. Tropomyosins (Tms), along with actin, are integral components of the microfilament cytoskeleton, although not all actin filaments have Tms bound to them (Bamburg, 1999). Tms bind largely by electrostatic charge to the helical groove of the actin filament and the >40 isoforms are obtained by alternative splicing from four genes, of which almost all are nonmuscle variants (Lees-Miller *et al.*, 1990; Goodwin *et al.*, 1991; Beisel and Kennedy, 1994; Dufour *et al.*, 1998; Cooley and Bergtrom, 2001). Although a considerable amount of information exists as to the biochemical regulation of microfilament dynamics, little is known about the function of this large family of proteins in vertebrate nonmuscle cells.

In vitro studies have shown that nonmuscle Tms are able to differentially protect actin from the severing action of gelsolin (Ishikawa *et al.*, 1989) and can regulate the Mg-ATPase activity of myosins to varying degrees (Fanning *et al.*, 1994). The different binding strengths to actin are thought to impart a range of stability to the filaments (Matsumura and Yamashiro-Matsumura, 1985; Hitchcock-DeGregori *et al.*, 1988; Pittenger *et al.*, 1995). The impact of Tms on vertebrate cell morphology is poorly understood even though studies suggest the importance of Tm isoforms in regulating

Article published online ahead of print. Mol. Biol. Cell 10.1091/mbc.E02–04–0244. Article and publication date are at www.molbiolcell.org/cgi/doi/10.1091/mbc.E02–04–0244.

Corresponding author. E-mail address: Ron.Weinberger@proteomesystems.com.au.
@ Present address: Proteome Systems, Ltd., North Ryde, New South Wales Z670, Australia.

myosin function and by implication, cell contractility. Overexpression of Tms 3 and 5 in CHO cells showed no effect on cell morphology or cytokinesis, although a chimeric Tm made of regions of both of these Tms caused multinucleation and cytokinetic defects (Warren *et al.*, 1995). Tm1 is the only naturally occurring Tm shown to have an impact on morphology. This Tm can restore stress fibers in oncogene transformed fibroblasts and increases cell spreading (Prasad *et al.*, 1993). The best evidence to date on unique functions of isoforms comes from mutant yeast studies. These studies have shown that one of the two yeast Tm isoforms is involved in the maintenance of actin cables and vesicle transport, and its absence provides a partial defect in polarized growth, whereas the smaller of the two isoforms is involved in axial budding. The two Tms were shown to have essential though noninterchangeable functions (Drees *et al.*, 1995).

Tms have been shown to be spatially and temporally regulated within cells, supporting the notion for unique functions. This is seen most dramatically within developing neurons where $Tm5_{NM1/2}$ is initially localized to the neuronal axon and later is replaced by the neuronal specific TmBr3 (Weinberger *et al.*, 1996). Even the neuronal growth cone has multiple domains characterized by the distribution of Tm isoforms that in part correlate with a specific structural organization of actin (Schevzov *et al.*, 1997).

The purpose of this study was to address whether Tm isoforms are able to spatially specify actin filament function. One mechanism by which Tms may function is by recruiting and/or regulating the activities of other actin-binding proteins. Lehman *et al.* (2000) have shown that Tm isoforms bind to different sites along the actin polymer and they have suggested that this may regulate the binding of other actin-binding proteins (Lehman *et al.*, 2000). Myosin is an obvious candidate based on the in vitro studies as well as its well-known regulation by troponin and Tm in the sarcomere. The phosphorylation of the regulatory light chains (MLC) of myosin II plays a critical role in controlling actomyosin contractility in both smooth- and nonmuscle cells (Chrzanowska-Wodnicka and Burridge, 1996). The ser-19 site on MLC is phosphorylated primarily by myosin light chain kinase (MLCK; Tan *et al.*, 1992) as well as Rho-kinase (ROCK) (Amano *et al.*, 1996) and is thought to control structural changes in the myosin tail resulting in the formation of myosin-based stress fibers in cells (Chrzanowska-Wodnicka and Burridge, 1996). It is also thought to enhance the binding of the myosin head to the actin filament (Sellers *et al.*, 1981; Sellers, 1991; Trybus, 1991). Dephosphorylation is by a specific myosin phosphatase whose activity is also regulated by ROCK via the Rho GTPase pathway (Kawano *et al.*, 1999; Kimura *et al.*, 1996).

Another candidate for Tm regulation in vivo is actin-depolymerizing factor/cofilin (ADF). In vitro studies have shown the competition of ADF and Tm for actin binding (Bernstein and Bamburg, 1982; Nishida *et al.*, 1985; Arber *et al.*, 1998). ADF is an actin-binding protein that can regulate the "twist" of the actin filament (McGough *et al.*, 1997) and enhances the turnover of actin by enhancing the off-rate from the pointed ends of F-actin and severing actin filaments (reviewed in Bamburg, 1999). The phosphorylation of ADF by Lim kinases inactivates the protein preventing the binding of ADF to the actin polymer (Arber *et al.*, 1998; Yang *et al.*, 1998).

The present study shows that the Tm isoforms $hTm5_{NM1}$ and TmBr3 can differentially regulate cell shape, migration, and microfilament organization in the brain-derived neuroepithelial B35 cell line (Schubert *et al.*, 1974). We chose these isoforms for study because earlier localization and developmental studies in the brain suggested distinct functions for these Tms (Weinberger *et al.* 1996). We anticipated that the ability of the B35 cell line to undergo morphological differentiation (Schubert *et al.*, 1974) would make the cell line more responsive to alterations in the molecular composition of the cytoskeleton. TmBr3 overexpression in B35 cells induced a loss of stress fibers and concomitant lamellipodial formation, whereas $hTm5_{NM1}$ overexpression lead to increased stress fibers and a reduction in lamellipodia. These Tm isoforms are associated with actin filaments of different molecular composition, which are localized to distinct cellular regions. The findings indicate that Tm isoforms can be used to specify the functional properties of an actin filament and that spatial segregation of isoforms can lead to localized specialization of actin filament function.

MATERIALS AND METHODS

DNA Constructs

Human $Tm5_{NM1}$, rat TmBr3, and GFP cDNAs containing only the coding region were cloned into the pHβApr(sig$-$) vector under control of the human β-actin promoter and the sequence was verified (Temm-Grove *et al.*, 1996; Qin and Gunning, 1997).

Cell Culture

The rat cortical neuronal cell line B35 (Schubert *et al.*, 1974) and all stably and transiently transfected clones were maintained in DMEM (Invitrogen, Mt. Waverly, Australia) supplemented with 10% fetal bovine serum and 2 mM L-Glutamine at 37°C and 5% CO_2. Cells were transfected both stably and transiently using Lipofectamine 2000 according to manufacturer's instructions (Invitrogen). Transfected clones were selected using 1% geneticin (Invitrogen) and clones were maintained in 0.5% geneticin. Primary cortical neurons were prepared from 14.5-d-old embryos as previously described (Hannan *et al.*, 1995). In brief, the cerebral cortices from 14.5-d-old embryos were aseptically dissected, freed from the meninges, and treated for 15 min with 0.25% trypsin 0.15% DNase I (Roche Diagnostics, Castle Hill, NSW, Australia). The tissue was dissociated by passing through a glass pasteur pipette several times. The single cell suspension was plated onto poly-L-lysine (1 mg/ml in PBS, Sigma, Alorich, Castle Hill, Australia)-coated glass chamber slides and cultured in neurobasal medium containing 2 mM L-glutamine, B27, and N2 supplements (Invitrogen) at 37°C in a humidified atmosphere of 5% CO_2.

Motility Assays

The cell migration assay was performed as described (Berens *et al.*, 1994). In brief, teflon-preprinted microscope slides were coated with 25 μg/ml poly-D-Lysine for 5 min, allowed to air-dry, and washed three times with PBS. The cell sedimentation manifold was placed over the slide and 1-μl cell suspension (2000 cells) was added to the slide. The slides were incubated on ice for 1 h and then at 37°C, 5%CO_2 for 1 h. The manifold was then removed and phase contrast reference images (Leica, Heidelberg, Germany) were taken at 2, 6, 12, and 24 h after seeding. The area covered by the cells was quantified using Image-Pro plus Version 4.0 (Media Cybernetics, Silver Spring, MD). All values at 24 h were divided by the area at the 2-h time point to obtain a relative migration index. Significance was determined using the Student's *t* test.

Generation and Screening of Transgenic Animals

Human $Tm5_{NM1}$ under the control of the β-actin promoter was removed from vector sequences by digestion with *Kpn*I and *Eco*RI (Roche Diagnostics). Fertilized eggs were collected from superovulated FVB/NJ females on the day of mating, injected with the DNA, and transferred to pseudopregnant ARC/5 females on the same day according to standard protocols (Hogan *et al.*, 1994). Transgenic mice were screened by Southern blot analysis of DNA extracted from mouse tails, digested with *Sac*I (Roche), and probed with a 1-kb *Sac*I DNA fragment derived from the 5′ flanking region of the human β-actin promoter.

Fixation and Immunostaining of Mouse Brain

Adult mouse brains were fixed in 10% buffered formalin and embedded in paraffin wax. Parasagittal serial sections (5 μm) were deparaffinized and rehydrated, and nonspecific binding was blocked with 10% fetal bovine serum in PBS, pH 7.4. Primary antibodies were incubated at room temperature for 1 h. The sections were washed three times in PBS followed by 1-h incubation with the secondary antibody. The secondary antibodies used were alkaline phosphatase–conjugated goat anti-rabbit IgG (H+L) and alkaline phosphatase–conjugated goat anti-mouse IgG (H+L) (Jackson ImmunoResearch Laboratories, Inc., West Grove, PA). The slides were incubated for 10 min in a pH 9.5 buffer (0.1 M Tris-HCl, 50 mM $MgCl_2$, 0.1 M NaCl), and immunoreactivity was visualized by the nitro blue tetrazolium chloride (NBT)/5-bromo-4-chloro-3-indolylphosphate-*p*-toluidine salt (BCIP) color reagent system (Invitrogen).

Immunohistochemistry

Cells were grown on poly-D-Lysine coated coverslips at a density of 2×10^4 cells/cm^2. The cells were fixed with 4% paraformaldehyde and permeabilized with chilled methanol. The primary rabbit antibodies used include the following: WSα/9d antiserum (Weinberger *et al.*, 1996) used at 1:3000; WSα/9c antiserum (Weinberger *et al.*, 1996) used at 1:250; MHCIIA and MHCIIB antisera (Rochlin *et al.*, 1995) used at 1:500 and 1:250, respectively, were a kind gift of Robert Adelstein; ADF/cofilin (Bamburg and Bray, 1987) and PADF/cofilin (Meberg *et al.*, 1998) antisera used at 1:250; and PMLC antiserum (Matsumura *et al.*, 1998) used at 1:10. Mouse monoclonal antibodies used include the following: LC1 used at 1:3000 (Warren *et al.*, 1995); CG3 (total Tm5) used at 1:250 (Lin *et al.*, 1988); C4 total actin (Lessard, 1988) used at 1:500, a kind gift of Jim Lessard; β-actin (clone AC-74) used at 1:1000 (Sigma); TM311 used at 1:1000 (Sigma), and total myosin light chain (clone MY-21) used at 1:250 (Sigma). Secondary antibodies conjugated to alkaline phosphatase, Cy3 (Jackson ImmunoResearch Laboratories, Inc.), or Alexa Fluor488 (Molecular Probes, Eugene, OR) were used. Secondary antibodies used were fluorescein isothiocyanate (FITC)-conjugated rabbit anti-mouse IgG (H+L), lissamine rhodamine B sufonyl chloride (LRSC)-conjugated goat anti-rabbit IgG (H+L) (Jackson ImmunoResearch Laboratories). Coverslips were mounted onto slides with the antifade reagent 1,4-Diazabicyclo[2.2.2]octane (DABCO; Sigma).

Immunoblot Analysis

Cells were harvested at 75% confluency for protein analysis and proteins were extracted using the method described in Wessel and Flugge (1984). Protein concentrations were determined using a BCA protein assay kit (Pierce, Rockford, IL). Proteins were loaded onto 15% low bis acrylamide gels and transferred to Immobilon-P PVDF membrane (Millipore Corporation, Bedford, MA). PVDF blots were blocked with 5% low fat skim milk overnight. Primary antibodies were diluted in TTBS (100 mM Tris-HCl, 150 mM NaCl, 0.05% Tween 20). Blots were incubated with primary antibody for an hour at room temperature, followed by two 10-min washes with TTBS. The blots were incubated with secondary antibodies (alkaline phosphatase rat anti-mouse or goat anti-rabbit IgG; H+L; Jackson ImmunoResearch Laboratories) diluted in TTBS for an hour. After two 5-min washes with TTBS, the blots were incubated in equilibration buffer for 2 min (100 mM Tris, pH 9.5, 50 mM $MgCl_2$, 100 mM NaCl). The bands were detected using CSPD (Roche Diagnostics) and exposure to Fuji x-ray film. Bands were quantified using ImageQuant V3.3 densitometry software (Molecular Dynamics).

Image Capture and Analysis

Fluorescence images were captured using a Spot II-cooled CCD digital camera (Diagnostic Instruments, Inc.) mounted on an Olympus Bx50 microscope. Images were captured sequentially through FITC and LRSC filter sets. Image analysis was performed using Image-Pro plus Version 4.0 (Media Cybernetics). Area measurements were taken of 100 cells, process length measurements were taken of 30 processes, and 50 cell areas were measured for the transient transfections. Statistical analyses were performed using one-way ANOVA tests with a Duncan post hoc analysis on the SPSS program (SPSS Inc.).

Preparation of Detergent Soluble and Insoluble Fractions

Triton-soluble and -insoluble fractions were performed as previously described (Minamide *et al.*, 1997). In brief, cultured cells were washed free of medium with four washes of 4°C PBS and lysed in 10 mM Tris, pH 7.5, 2 mM $MgCl_2$, 0.5 mM DTT, 2 mM EGTA, 1% Triton X-100, and 7.5% glycerol. The cells were scraped off the dish and transferred to a centrifuge tube. Soluble and insoluble fractions were prepared by centrifugation of the lysates at $17{,}000 \times g_{max}$ for 20 min. Proteins were detected in each fraction by immunoblot analysis.

Immunoprecipitation

For immunoprecipitation, the relevant antibodies were bound to protein A-sepharose CL-4B beads (Sigma). Cells, 1×10^7, or 100 μg whole adult mouse brain were washed twice with PBS followed by lysis with RIPA buffer (1% Nonidet P-40, 0.1% SDS, 1% Na-deoxycholate, 10 mM Tris-HCl, pH 8, 140 mM NaCl, and complete mini-protease inhibitor EDTA-free (Roche). Cells were scraped off the plate and insoluble matter was removed by centrifugation. The cell lysates were added to 40 μl of antibody-bead solution and gently mixed for 3 h at 4°C. Proteins were extracted from the beads by boiling the samples to 95°C and separated by PAGE. After electroblotting onto PVDF, the separated proteins were identified using specific antibodies (ADF, LC1, WSα/9c, C4 total actin).

RESULTS

Stable Transfections Reveal Distinct Effects of $hTm5_{NM1}$ and TmBr3 on Cell Morphology and Migration

Plasmids containing the TmBr3 and $hTm5_{NM1}$ plasmids were transfected into B35 neuroepithelial cells. The resultant protein expression could be monitored by the antibodies LC1, which specifically identifies $hTm5_{NM1}$, and WSα/9c, which identifies TmBr3. Initially, we transiently transfected B35 cells with the Tm constructs and investigated cell morphology 24 h later. Our results showed that TmBr3 decreased cell surface area by 45 ± 8% (n = 100 cells), and $hTm5_{NM1}$ increased surface area by 50 ± 5% (n = 100 cells). To more accurately determine the relationship between Tm levels and morphological impact, we developed stably transfected clones expressing a range of levels of both TmBr3 and $hTm5_{NM1}$. Figure 1, m and n, shows the range of expression for both the isoforms. The lowest and highest expressors were selected for further investigation as well as

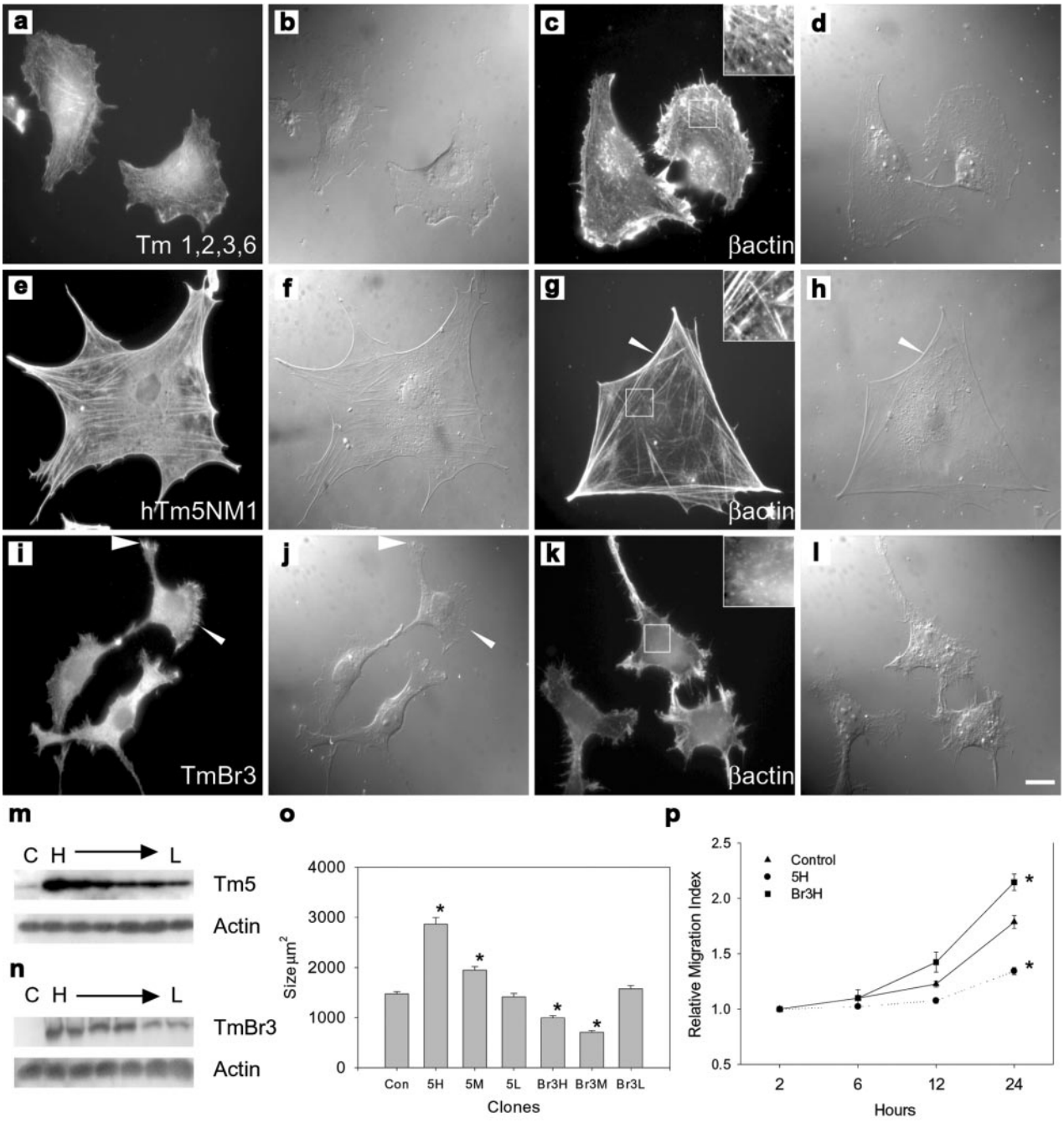

Figure 1. Tm isoforms impact on cellular morphology and the arrangement of the cytoskeleton. (a) Control B35 cells immunostained with Tm311 and β-actin (c) showing the presence of fine stress fibers (insert c). (e and g) $hTm5_{NM1}$ transfectants immunostained with LC1 (which only detects transfected $hTm5_{NM1}$) and β-actin, respectively. Large, well-organized stress fibers were seen throughout the cells (insert g); arrowhead indicates the arced membrane at the edge of the cell. (i and k) TmBr3 transfectants immunostained with WSα/9c (which detects only TmBr3 in these cells) and β-actin, respectively. Punctate, perinuclear localization of TmBr3 with accumulation in the cell periphery (arrowheads) was observed as well as a decrease in stress fibers (insert k). Corresponding differential interference contrast images are shown in panels b, d, f, h, j, and l. Scale bar 10 μm. m, Western blots of control cells (Con) and a range of high to low (H$\rightarrow$L) expressing $hTm5_{NM1}$ clones showing the increase in total Tm5 levels. Total actin levels remained unchanged. (n) Western blot of control cells and a range of high to low expressing TmBr3 clones showing the increase of TmBr3 levels in these clones; however, total actin levels remained unchanged. (o) Histogram showing the average surface areas of a range of high, moderate, and low expressing $hTm5_{NM1}$ and TmBr3 clones compared with control cells. Cell area measurements were taken of 100 cells per clone. *$p < 0.05$. p, Graph showing the increase in relative migration index of the Br3H cells compared with the control B35 cells as well as the decrease in motility seen in the 5H cells. There were no differences seen in the number of cells over the 24-h period. *$p < 0.05$ n = 9 (measurements of each cell line at each time point).

a clone that expressed approximately midway between these points. The clones have been termed L, H, and M, respectively. Northern blot analysis using a probe that recognized a region common to both exogenous mRNAs revealed that the TmBr3 clones expressed at lower levels than the $hTm5_{NM1}$ clones although there was considerable overlap. The highest level of exogenous $hTm5_{NM1}$ mRNA was set at 100%. In comparison to this value, Tm expression ranged from 18–100% for the $hTm5_{NM1}$ clones and 3–73% for TmBr3 clones. These results indicate that any differences observed between the TmBr3 and $hTm5_{NM1}$ clones could not simply be accounted for by a difference in exogenous Tm mRNA levels.

Figure 1, a–l, shows the impact of the Tms on cell morphology as well as microfilament organization in the highest expressing clones. 5H clones were large with long, well-defined stress fibers spread throughout the cytoplasm (Figure 1g) into which $hTm5_{NM1}$ incorporated (Figure 1e). The cells had arced membranes as visualized by differential interference microscopy (DIC) that appeared to be under significant tension (arrowhead, Figure 1, g and h) and rarely showed lamellipodia, which was in direct contrast to control cells (Figure 1, a–d). The stable transfectants appeared to reproduce the morphological effect seen with transient transfection of $hTm5_{NM1}$ (unpublished data).

In contrast to the 5H, Br3H cells were smaller than control cells and had a diffuse distribution of actin with very few detectable stress fibers (Figure 1, k and l). In addition, TmBr3 was localized in a perinuclear manner with some localized concentrations at the cell periphery (arrowheads, Figure 1, i and j). Again, these results were very similar to that seen in the transient transfections (unpublished data).

Impact on cell surface area was largely related to the levels of hTm5NM1 and TmBr3. Figure 1o shows that 5H was almost twice the size of control cells with surface area decreasing to control levels in 5L. Similarly, both the Br3H and Br3 M clones were ~35% smaller, whereas Br3L was similar to controls. Migration assays were performed to determine whether alterations in actin filament organization had an impact on motility. Figure 1p revealed that at 6 h postplating no differences were observed in the migration of Br3H and 5H cells. However, at 12 h significant differences in the area covered by the cell lines were observed. At 24 h, Br3H cells had covered an area almost twice that of 5H cells. 5H cell migration was reduced by 25% relative to controls, whereas Br3H cells migrated further by 24%. These findings indicate that the Tm isoform specific effects on actin filament organization and cellular morphology have a direct impact on the functional properties of the B35 cells.

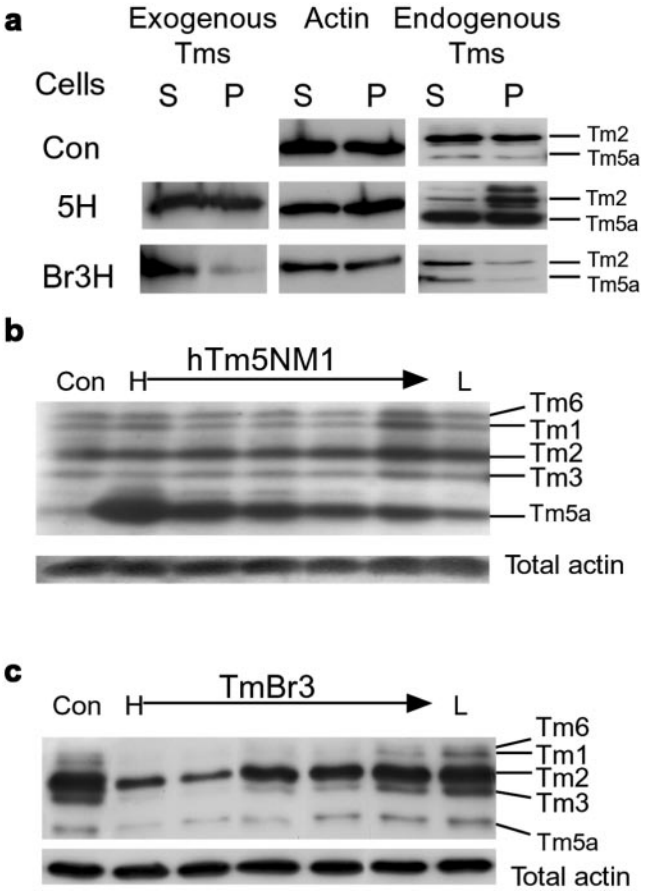

Figure 2. Expression of exogenous Tm isoforms alters the biochemical properties and levels of endogenous Tm isoforms. (a) Triton extraction and ultracentrifugation of proteins from control cells, 5H and Br3H clones into triton soluble (S) and insoluble/pellet (P) fractions showed that the exogenous $hTm5_{NM1}$ was detected evenly between the soluble and insoluble fractions, whereas the majority of the exogenous TmBr3 is in the triton-soluble fraction indicating that it is not associated with large stress fibers. Total actin was detected evenly between S and P for all cell types that demonstrates that there was no change in the soluble:pellet actin ratios. The overexpression of $hTm5_{NM1}$ increased the amount of endogenous Tm isoforms in the P fraction compared with the control cells and TmBr3 cells, indicating that the endogenous Tm isoforms are associated preferentially with stress fibers and small filaments. (b) Increasing $hTm5_{NM1}$ expression was associated with an increase in Tm5a expression. There was no change in the levels of HMW Tms (Tm6, 1, 2, and 3) and total actin levels remained unchanged. (c) TmBr3 overexpression results in decreased HMW Tm levels. Total actin levels remained unchanged.

Increased $hTm5_{NM1}$ and TmBr3 Levels Alter Expression of Other Tms as well as Their Biochemical Partitioning and Localization

A possible explanation of $hTm5_{NM1}$ action is that it increases stress fiber formation by either increasing actin polymer levels and/or total actin. Figure 2, b and c, shows that levels of total actin remained unchanged. This suggests that the level of Tm-bound actin filaments is increased in these cells. Detergent extraction and centrifugation was performed to fractionate the actin populations. The relatively low speed of centrifugation ensured that actin monomer as well as small polymer and oligomer were present in the detergent soluble phase (Figure 2a). The fraction of pelletable actin observed in control and 5H cells was 50%. Therefore, $hTm5_{NM1}$ does not appear to act by significantly increasing the large polymer pool or total actin level. This is supported by exposure of B35 cells to the actin polymer stabilizing drug jasplakinolide, which did not reproduce the $hTm5_{NM1}$ phenotype (unpublished data). Similarly, total actin levels did not alter in the TmBr3 clones regardless of expression level. In Br3H,

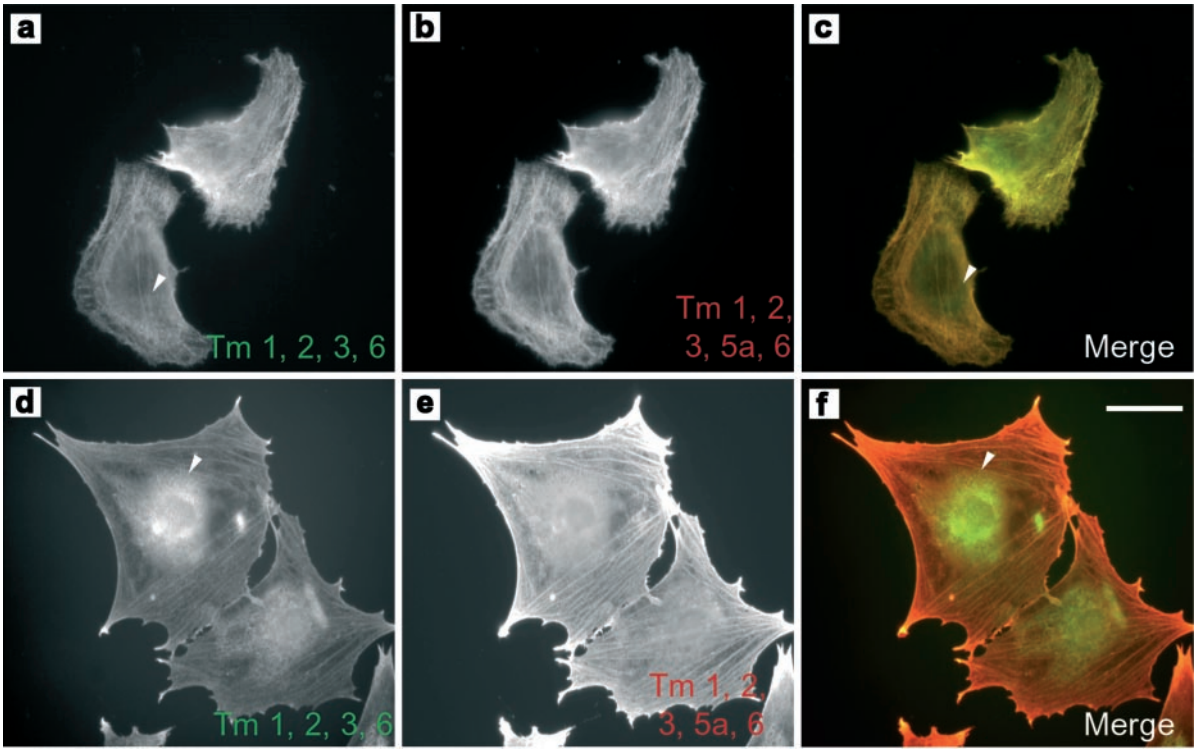

Figure 3. $hTm5_{NM1}$ can regulate the molecular composition of stress fibers. Control B35 cells were immunostained with TM311 to visualize the stress fibers containing the high molecular weight Tms 1, 2, 3, and 6. Arrowhead indicates the absence of perinuclear staining (a). The HMW Tms and Tm5a were detected using the WSα/9d antibody showing that Tm5a is also localized to stress fibers (b). (c) Merge of a (green) and b (red). (d) 5H immunostained with TM311. A subset of HMW Tms is localized in a punctate perinuclear manner (arrowhead). (e) Tm5a is localized predominantly to stress fibers in Tm5H cells as detected by the WSα/9d antibody. (f) Merged image of d (red) and e (green). Scale bar, 15 μm.

actin partitioned in a similar manner to that of controls even though large stress fibers were absent from these cells (Figure 2a). Therefore, although actin filament organization has been altered in both sets of clones, this is not reflected in a major change in the biochemical fractionation of actin or its levels.

The lack of major alterations in the fractionation of actin suggested that effects of the Tms may be exerted within subpopulations of the actin filament system. The composition of specific subpopulations of actin filaments as identified by Tm isoforms, was altered. The exogenous Tms segregated differently. TmBr3 was present predominantly in the soluble fraction (Figure 2a), whereas $hTm5_{NM1}$ was equally distributed between the two fractions (Figure 2a). Constitutively expressed TmBr3 and $hTm5_{NM1}$ altered levels of endogenous Tms as well. Tm5a increased in $hTm5_{NM1}$ transfected clones in a dose-dependent manner, whereas Tms 1, 2, 3, and 5a were downregulated in TmBr3-expressing clones (Figure 2, b and c). The HMW Tms are generally associated with stress fibers (Lin *et al.*, 1988), and the reduction of these Tms as well as Tm5a may contribute to the lack of stress fibers in TmBr3-expressing clones.

Endogenous Tm5a appeared predominantly in the soluble fraction in Br3H cells, whereas this isoform was equally distributed between the soluble and pellet fractions in 5H cells. Tm2 was found to be equally distributed between the soluble and pellet fractions of control cells and almost entirely in the pellet fraction of 5H cells. Surprisingly, this altered distribution of the high molecular weight (HMW) isoform Tm2 is not due to recruitment into stress fibers. Figure 3 shows staining of the HMW Tms 1, 2, 3, and 6, with the Tm311 antibody in 5H and control cells (Figure 3, d and a, respectively). The HMW Tms are found on stress fibers and also diffusely organized in control cells. This distribution is identical to the localization seen with another antiserum that also identifies the LMW Tm5a (Figure 3b). In 5H cells the HMW Tms are found most enriched in granular aggregates surrounding the nucleus (Figure 3d, arrowhead), although weak staining of stress fibers is also seen within the cytoplasm. This perinuclear pattern of staining is not seen in control cells (Figure 3, a vs. d). In contrast the antibody, which recognizes both HMW Tms and Tm5a, shows strong stress fiber staining (Figure 3e), suggesting that Tm5a is preferentially recruited to these structures. This selective exclusion of the HMW Tms from stress fibers is consistent with in vitro and tagged Tm transfection data that revealed poor dimerization of $hTm5_{NM1}$ with these Tms (Temm-Grove *et al.*, 1996). The same studies showed a strong preference for heterodimerization with Tm5a that is consistent with its coincorporation into stress fibers in the 5H cells. Therefore, $hTm5_{NM1}$ and TmBr3 are able to alter the associ-

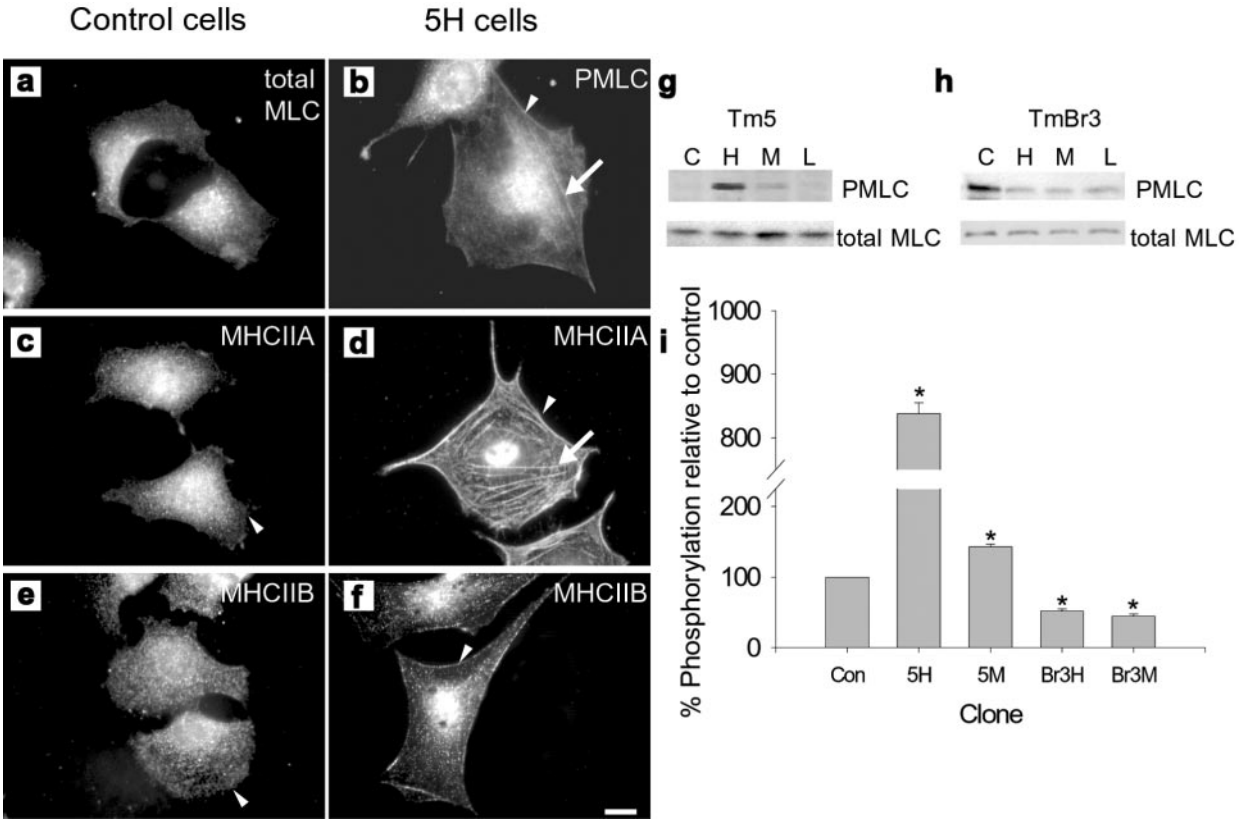

Figure 4. Tm isoforms can alter the activity and cellular localization of myosin II. Perinuclear localization of phosphorylated myosin light chain (PMLC) was observed in control cells (a), whereas in 5H (b) PMLC was localized to stress fibers (arrow) and the periphery of the cell (arrowhead). Myosin heavy chain IIA (MHCIIA) localization in control cells (c) was diffuse throughout the cytoplasm, but it was not present at the edge of the cell; however, in 5H (d) MHCIIA was localized to large stress fibers throughout the cell (arrow) as well as at the cells periphery (arrowhead). In control cells (e), myosin heavy chain IIB (MHCIIB) localization was punctate throughout the cytoplasm, whereas in 5H (f) there was an enrichment of MHCIIB at the cell periphery (arrowhead). Scale bar, 10 μm. (g) Western blots showing the levels of phosphorylated myosin light chain (PMLC) and total myosin in control (C), high (H), moderate (M), and low (L) expressing $hTm5_{NM1}$ (g) and TmBr3 clones (h). These levels were quantified relative to control levels and shown in the histogram (i); *$p < 0.05$.

ation of endogenous Tm isoforms with biochemically and immunohistochemically distinct microfilament populations.

$hTm5_{NM1}$ Overexpression Can Recruit Myosin II to Stress Fibers

The ability of $hTm5_{NM1}$ and TmBr3 to regulate stress fiber formation strongly suggested that myosin II may be involved. Burridge and coworkers (Chrzanowska-Wodnicka and Burridge, 1996) have proposed that myosin II–based contractility is the force that drives assembly of stress fibers. Figure 4, c and e, shows that in control cells neither of the myosin heavy chain isoforms IIA or IIB (MHC IIA or MHC IIB) are colocalized with stress fibers, and both show a diffuse and predominantly punctate distribution with some perinuclear staining. This was surprising, considering that the control B35 cells contain stress fibers. Incorporation of $hTm5_{NM1}$ into stress fibers specifically recruits MHC IIA but not IIB into these structures, with the majority of MHC IIA staining now present on stress fibers (Figure 4d). Although not incorporated into stress fibers, MHC IIB now shows enriched deposits at the cell periphery that are not seen in control cells (Figure 4f, arrows).

In smooth and nonmuscle cells, phosphorylation of the regulatory light chain of myosin II is believed to promote the contractility and stability of actomyosin by stimulating the actin-activated ATPase activity (Sellers *et al.*, 1981). Accompanying the MHC IIA presence in 5H stress fibers was the accumulation of phosphorylated myosin light chain (PMLC) in these structures (Figure 4b). This supports the active contractility of MHC IIA in the $hTm5_{NM1}$-containing stress fibers. The degree of PMLC was quantitated by an antiserum that specifically recognizes the phosphorylated ser-19 of the regulatory light chain of myosin II and showed a dose-dependent correlation with the level of $hTm5_{NM1}$ (Figure 4g). PMLC was about 8-fold greater than controls in the 5H clones and 1.5-fold greater in the 5M clones (Figure 4i). In contrast, Br3H and Br3 M clones showed an ~50% decrease in PMLC levels (Figure 4, h and i). The findings suggest that $hTm5_{NM1}$ stimulates stress fiber formation in B35 cells in a dose-dependent manner by recruiting myosin II into stress fibers, which have increased contractility leading to larger

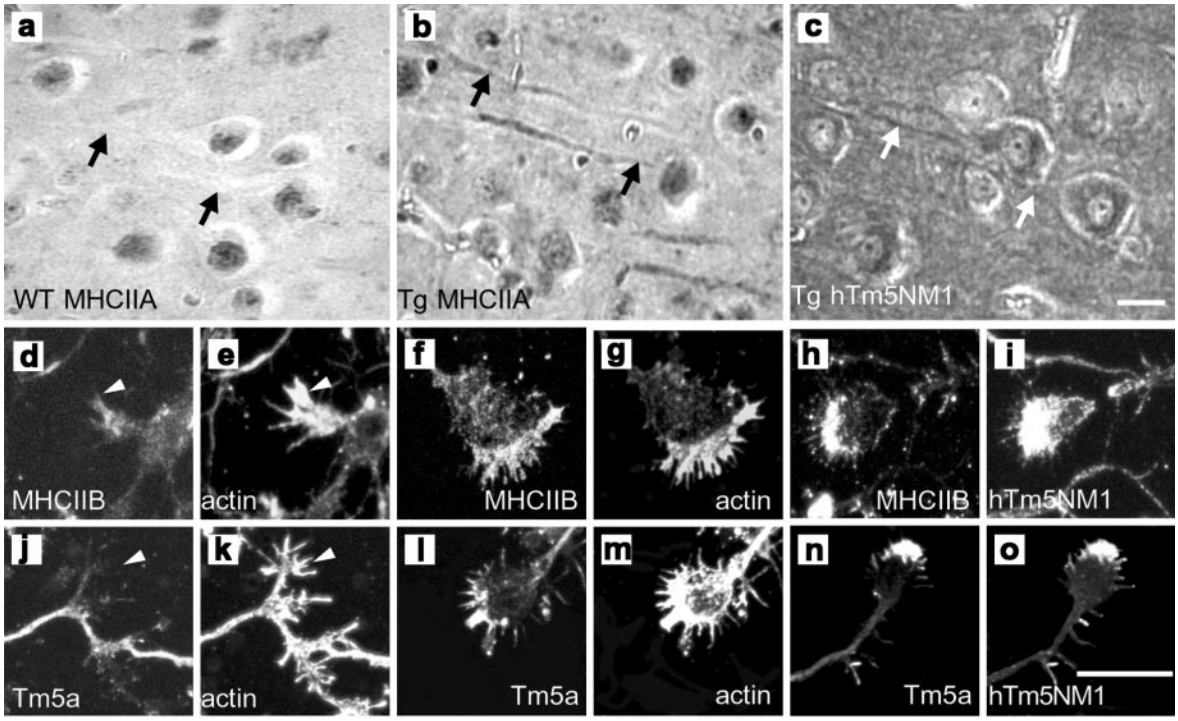

Figure 5. Overexpression of Tm isoforms in vivo results in altered actin organization and myosin localization. Ectopic expression of $hTm5_{NM1}$ alters the spatial intracellular segregation of myosin isoforms IIA, IIB and Tm isoforms. Immunohistochemistry of 10 μm thin parasaggital sections of (a) wild-type and (b and c) $hTm5_{NM1}$ transgenic adult mouse cortex, incubated with myosin IIA (a and b) and LC1 antibodies (c). Myosin IIA is present predominantly in the dendrites and cell bodies of $hTm5_{NM1}$ overexpressing cortical neurons (b and c), respectively; see arrows. Arrows in a indicate the lack of myosin IIA in the dendrites and cell bodies of control cortical neurons. Scale bar, 10 μm. Confocal microscope images of immunofluorescence stained in vitro cultured 5-d-old primary cortical neuron growth cones. Control growth cones were double-immunostained with myosin IIB and actin (d and e) and WSα/9d and actin (l and k), respectively. $hTm5_{NM1}$ overexpressing growth cones were double-immunostained with myosin IIB and actin (f and g), myosin IIB and LC1 (h and i), WSα/9d and actin (l and m), WSα/9d and LC1 (n and o), respectively. Myosin IIB is enriched in the growth cone periphery of $hTm5_{NM1}$ over expressing cortical neurons (f and h), where the exogenous $hTm5_{NM1}$ protein detected with the LC1 antibody is also present (i), this staining pattern is not obviously seen in control growth cones (d and e). Tropomyosin isoforms detected with the WSα/9d antibody were also found enriched in the growth cone periphery (i and k), where the exogenous $hTm5_{NM1}$ is also present (o). In control growth cones the Tm isoforms detected with the WSα/9d antibody are highly diminished (j and k). Scale bar: (d–o), 10 μm.

cells. TmBr3, however, appears to drive the formation of smaller actin filaments that have a reduced myosin II phosphorylation (Figure 4h).

$hTm5_{NM1}$ can also induce changes in the localization of myosin in intact brain tissue and primary embryonic cortical neurons in culture. Expression of $hTm5_{NM1}$ in mouse cerebral cortex results in its localization in the somatodendritic compartment of pyramidal neurons (Figure 5c). This is accompanied by the localization of MHCIIA to the dendrites (Figure 5b), a location not observed in control littermates (Figure 5a).

Primary embryonic cortical neurons derived from these transgenic mice expressing $hTm5_{NM1}$ display significantly enlarged growth cones reminiscent of the increase in cell size seen in the B35 cells (Schevzov *et al.*, manuscript in preparation). The $hTm5_{NM1}$ is enriched in these growth cones and extends well into the filopodia (Figure 5i). MHC IIB (Figure 5, f and h) but not MHC IIA (unpublished data) is localized in the filopodia and the leading edge of the growth cone, from which it is absent in control animals (Figure 5, d and e). Previously, Tm5a was seen colocalized with $hTm5_{NM1}$ in transient and stably transfected B35 cells. Tm5a colocalizes with $hTm5_{NM1}$ in the growth cones of transgenic neurons (Figure 5, n and o), whereas it is barely detectable in the growth cones of control littermates (Figure 5j). These findings show that there is a relocation of both myosin IIB and Tm5a in $hTm5_{NM1}$ transgenic neurons, which recapitulates events seen in the B35 cells.

$hTm5_{NM1}$ Can Displace ADF from Actin Filaments

ADF/cofilin is a well-studied regulator of actin filament dynamics that has been shown to increase filament turnover and is thought to compete with certain Tm isoforms for binding to actin filaments in vitro (Bernstein and Bamburg, 1982; Nishida *et al.*, 1985). Unbound/displaced ADF is phosphorylated by Lim kinases, which inactivates the protein, leading to more stable actin filaments (Arber *et al.*, 1998; Yang *et al.*, 1998). Levels of phosphorylated ADF are therefore a good marker of inactive/unbound ADF. Figure 6 shows the levels of phosphorylated, inactive ADF (PADF) in the $hTm5_{NM1}$ (Figure 6a) and TmBr3 clones (Figure 6b).

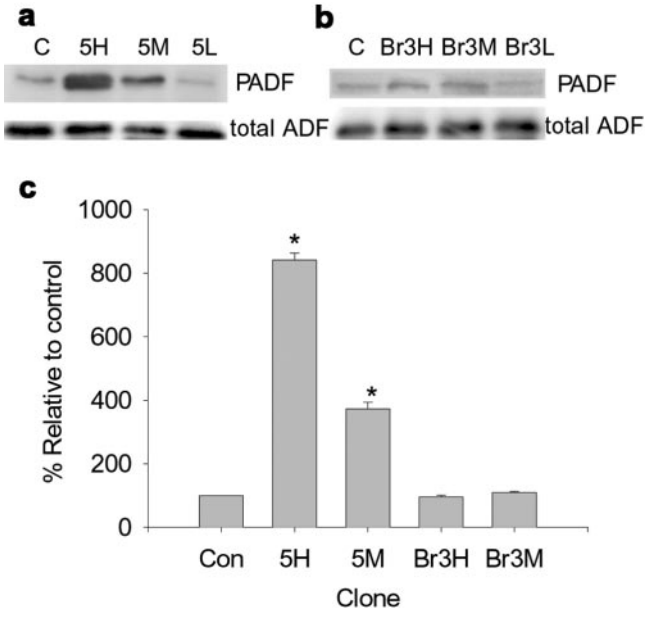

Figure 6. Expression of $hTm5_{NM1}$ but not TmBr3 alters the activity of actin depolymerizing factor. Western blots showing the levels of phosphorylated ADF/cofilin (PADF) and total ADF levels in control cells and high, moderate and low expressing $hTm5_{NM1}$ (a) and TmBr3 clones (b). The graph (c) shows the quantification of PADF levels with respect to control levels. *$p < 0.05$.

$hTm5_{NM1}$ increased the fraction of PADF 8- and 3-fold in the Tm5H and Tm5 M clones, respectively, whereas no alterations were seen in the Br3H and Br3 M cell lines. This suggests that expression of $hTm5_{NM1}$ correlates with the displacement of ADF from actin filaments. This isoform specific effect is consistent with an increased stability of actin filaments in $hTm5_{NM1}$ cells that leads to an altered morphology.

TmBr3 Can Induce Lamellipodia and Is Associated with ADF Containing Actin Filaments

A possible explanation for the absence of prominent stress fibers seen in the TmBr3 clones is the observed decrease in the actin-stabilizing HMW Tms. To test this hypothesis we transiently cotransfected the TmBr3 vector with a plasmid encoding GFP, which was used as a transfection marker, into 5H cells. This cell line has stress fibers that are predominantly free of HMW Tms. Therefore, any alterations to stress fibers that resulted from TmBr3 transfection cannot not be accounted by the loss of HMW Tms from these structures.

Figure 7a shows cells immunostained with β-actin following transfection, and Figure 7b identifies the cells expressing the GFP marker. The large untransfected 5H cell contains distinct stress fibers, whereas the GFP tagged cells were dramatically diminished in size and show prominent lamellipodia that are very highly enriched in β-actin, whereas $hTm5_{NM1}$ containing stress fibers are absent in the transfected cells (Figure 7, d and e). No reduction in levels of other Tms was observed even though >40% of cells were transfected (unpublished data). Quantitative analysis shows that TmBr3-transfected cells had a $55 \pm 4\%$ ($n = 50$; $p < 0.01$) smaller surface area than untransfected Tm5H cells. We conclude that the loss of stress fibers as a result of TmBr3 expression appears to be independent of the Tm isoform composition of the actin filaments.

In control and Br3H cells ADF is primarily localized to the perinuclear region as well as lamellipodia where increased motility and actin filament turnover would be expected (arrowheads, Figure 8, a and c). In contrast ADF is absent from the edges of 5H cells (arrowhead, Figure 8b). TmBr3-transfected 5H cells show the relative absence of stress fibers and the deployment of β-actin to lamellipodia (Figure 8e). ADF is most enriched ~5 μm away from the leading edge, although staining was present throughout the lamellipodium (Figures 8d, arrowheads, and 9a) and overlaps with β-actin localization (Figure 8f, arrowheads). This has previously been observed in fish keratinocytes where ADF is involved in the disassembly of actin filaments behind the highly branched ARP2/3 containing actin filaments (Svitkina and Borisy, 1999). TmBr3 localizes to lamellipodia (Figure 9, b, d, e, and h) and the nuclear region and shows an almost identical pattern of staining to β-actin in lamellipodia (Figure 9, e–g). There is an overlap of localization of ADF and TmBr3 in the lamellipodium (Figure 9. a–c). TmBr3 extends to the leading edge of the lamellipodium (Figure 9, b and e, inset, and d and h); however, it is not present in the filopodia.

The immunolocalization studies in Figure 9 suggested that TmBr3 might be bound to ADF-containing filaments. To test this we used the WSα/9c antiserum to immunoprecipitate TmBr3 from Br3H cells in the hope of pulling down a complex that also contained actin and associated proteins (Figure 10). The WSα/9c immunoprecipitate contained TmBr3 and actin as well as ADF. This finding was confirmed by immunoprecipitation from brain (Figure 10b). Control immunoprecipitation in the absence of primary antiserum failed to bind any of these proteins. In contrast LC1, the mAb that specifically binds to $hTm5_{NM1}$, immunoprecipitated $hTm5_{NM1}$ and actin from Tm5H cells but not ADF even though there was strong ADF immunoreactivity in the cell lysate (Figure 10a). Similarly, ADF could not be coimmunoprecipitated from mouse brain using the CG3 antibody that interacts specifically with Tm5 from rodent and human. This suggests a specific interaction of ADF with TmBr3 containing filaments and not $Tm5_{NM1}$ filaments.

DISCUSSION

Tms Can Incorporate into Specific Cellular Compartments with Structurally Distinct Actin Filaments

There is now ample evidence that Tms identify unique, multiple actin filament populations. The most detailed studies have been performed in the nervous system where Tm isoforms specify neuronal compartments such as the axon, somato-dendritic, and the highly motile growth cones (Gunning *et al.*, 1998a). The growth cone actin filament population can be further subdivided into three Tm distinguishable groups related to specific structural regions (Schevzov *et al.*, 1997). The microcompartmentation is most effectively highlighted at the synapse where Tm4 is postsynaptic and

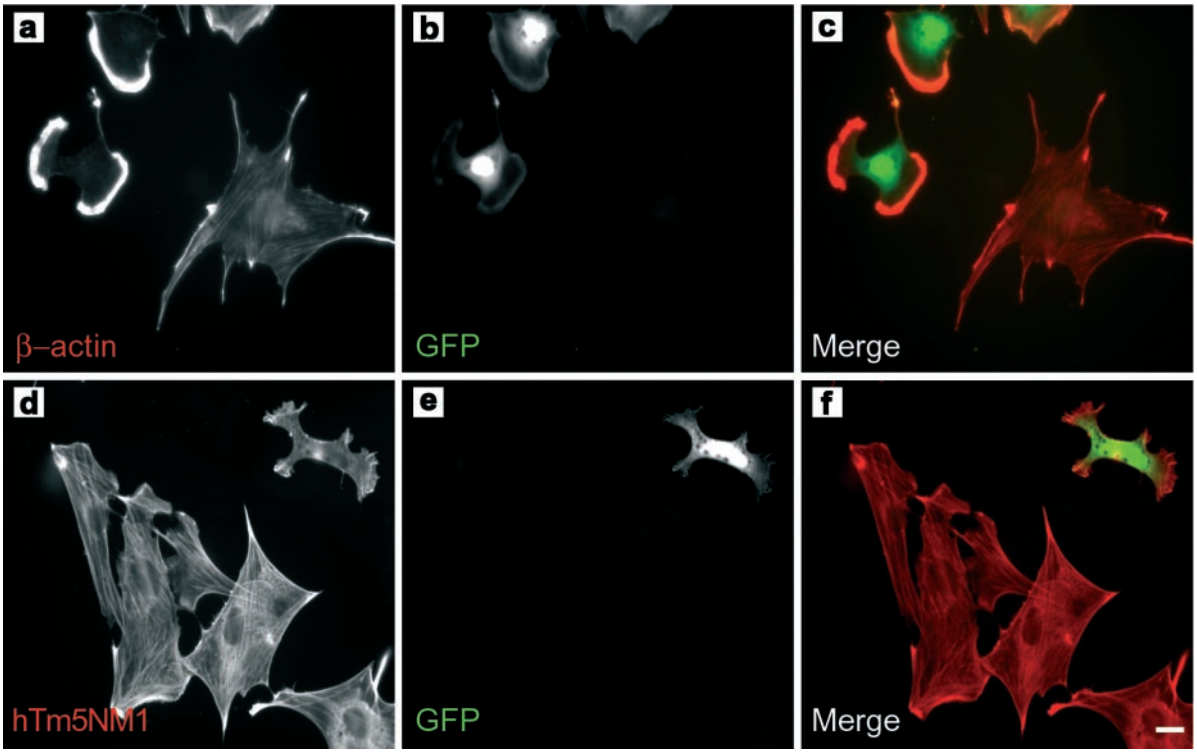

Figure 7. Transient expression of TmBr3 can impact on the size of the cell and the arrangement of actin. 5H was transiently cotransfected with TmBr3 and GFP. (a) β-Actin immunostaining revealed that the cotransfected cells underwent drastic actin rearrangements with the loss of the large stress fibers seen in untransfected cells and the formation of β-actin rich lamellipodial regions. (b) GFP expression. (c) Merged image of a (red) and b (green). (d) Untransfected and transiently cotransfected 5H cells immunostained with LC1. $hTM5_{NM1}$ stress fibers were not present in 5H cells cotransfected with TmBr3 and GFP. (e) GFP expression. (f) Merged image of d (red) and e (green). Scale bar, 10 μm.

TmBr3 is primarily presynaptic (Had *et al.*, 1994). This actin filament compartmentation is not unique to the nervous system and actin filament populations distinguished by Tm isoforms have been found to be associated with golgi-derived vesicles in fibroblasts and whole liver (Heimann *et al.*, 1999), the cytokinetic machinery of mitotic astrocytes (Hughes *et al.*, 2002) and basolateral and apical surface of epithelial cells (Percival *et al.*, 2000). Tms are present within motile regions such as lamellipodia (Lin *et al.*, 1988), where actin filaments are more dynamic as well as more stable structures such as the cortical network of red blood cells (Sung *et al.*, 2000) and stress fibers (Pittenger and Helfman, 1992). Each of these compartments contains actin filaments with different structural properties and the localization data suggests the possibility of specific functions of Tms in these cellular regions. With >40 isoforms identified (Miller *et al.*, 1990; Goodwin *et al.*, 1991; Beisel and Kennedy, 1994; Lees-Dufour *et al.*, 1998; Cooley and Bergtrom, 2001) and only a tiny fraction of these examined in cell biological studies, it is essential to use panels of antibodies with defined specificities to accurately determine localization.

The present studies have demonstrated the ability of Tm isoforms to incorporate into distinct cellular regions and specific actin filament structures of B35 cells. TmBr3 incorporated into filaments of lamellipodia, whereas Tm5 incorporated into stress fibers of the cytoplasm. Detergent extraction revealed a distinct partitioning of these Tms, further supporting their association with different cytoskeletal structures. The localization of TmBr3 to the leading edge supports the findings of other groups that have identified Tms at lamellipodia (Lin *et al.*, 1988) and our work in growth cones (Schevzov *et al.*, 1997). In fact, in the primary cortical neurons of Tm5 transgenic mice shown in this study, both Tm5 and Tm5a were colocalized to the furthest edge of growth cones. The finding that these Tms can incorporate into the stress fibers of B35 cells as well as the dynamic microfilaments of the growth cone suggest that the use of Tms is context dependent. The context may vary during a cell's life cycle and between cell types. This may be dependent to some extent on the availability of other Tms or other actin/Tm binding proteins.

Tms Can Alter Actin Filament Organization, Which Leads to Unique Cellular Morphologies

The most striking differences of the Tms was their ability to differentially regulate cell morphology. Cell surface area was the most noticeable readout of the transfections, with $hTm5_{NM1}$ consistently increasing cell surface area and TmBr3 decreasing it. Another obvious difference observed by light microscopy was the inhibition of lamellipodia in $hTm5_{NM1}$-transfected cells and a promotion of lamellipodia

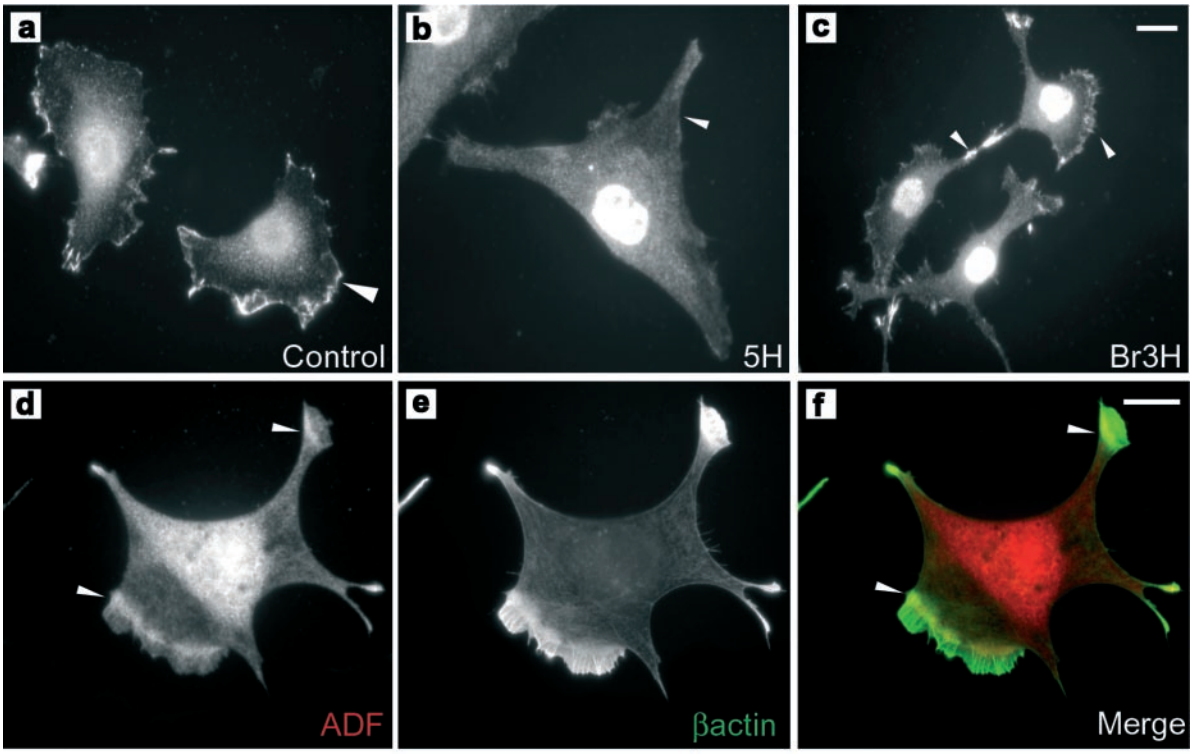

Figure 8. The molecular composition of the actin microfilament alters the localization of ADF. ADF was highly enriched at the cell periphery in control cells (a) and Br3H cells (c); however, this enrichment was not seen in 5H cells (b). Transient transfection of TmBr3 into 5H cells alters the localization of actin depolymerizing factor. ADF has been relocalized to just behind the β-actin rich lamellipodial region and to the tips of processes (arrowhead) (d). (e) β-Actin was localized to the lamellipodial regions and to the tips of the processes. (f) Merged image of d (red) and e (green). Scale bar, 10 μm.

by TmBr3. The ability of TmBr3 to promote lamellipodia was visualized three ways in the B35 cells: by transient transfection into B35 cells, transient transfection into 5H cells, and stable expression in isolated clones. Although stable clones showed a decrease in Tm isoform levels in response to constitutive TmBr3 expression, the loss of stress fibers could still be achieved in TmBr3 transient transfections, where the levels of other Tms were not affected or the Tm composition of stress fibers had been altered. The findings indicated that the effect of TmBr3 was dominant irrespective of the Tm composition of stress fibers.

The properties conferred to the actin filaments by the Tm isoforms resulted in changes to cellular motility. This finding indicates that the cellular and cytoskeletal changes induced by the Tm isoforms can alter the functional properties of cells. Inhibition of a Tm δ-gene product has also been reported to regulate melanoma cell motility (Miyado *et al.*, 1996). In the B35 cells a reduction in stress fibers correlated with increased motility. Lamellipodial formation has been observed to accompany stress fiber turnover in migrating cells, similar to that seen for TmBr3. The contrasting effects on motility between the Tm isoforms suggests that changes in the balance of Tm isoforms within a cellular compartment may have an impact on the ability of a cell to migrate in situ. In this regard, the Br3H and 5H cells also showed altered regulation of other Tm isoforms. $hTm5_{NM1}$ showed an induction and possible dimerization with Tm5a (Gimona *et al.*, 1995; Temm-Grove *et al.*, 1996), excluding HMW Tms from stress fibers, which may have also contributed to the functional changes observed. The spatial and temporal regulation of Tm isoform expression observed in CNS development, where migrating/mitotic cells differ significantly in their expression of Tm isoforms (Stamm *et al.*, 1993; Weinberger *et al.*, 1996; Hughes *et al.*, 2002), may contribute to cell migration and the development of brain structure. The large number of Tm isoforms identified suggest the possibility that the choice of Tm isoforms most appropriate for motility from one cell type to the other may be cell or tissue type specific. Ultimately, the balance of Tm isoforms and their targeting rather than the expression of one or other isoform is likely to determine specific cellular properties.

The polymeric state of the cytoskeleton has been shown to impact on the activities of the actin filament regulating GTPases of the Rho family (Ren *et al.*, 1999). The structural impact of $hTm5_{NM1}$ is similar to that observed in cells that have activated Rho (Ridley and Hall, 1992), whereas that seen in the TmBr3 cells was reminiscent of Rac 1 effects (Ridley *et al.*, 1992). It will be important to understand the whether the alterations in actin filament organization induced by altering Tm isoform levels within cells feeds back to regulate these central signaling pathways.

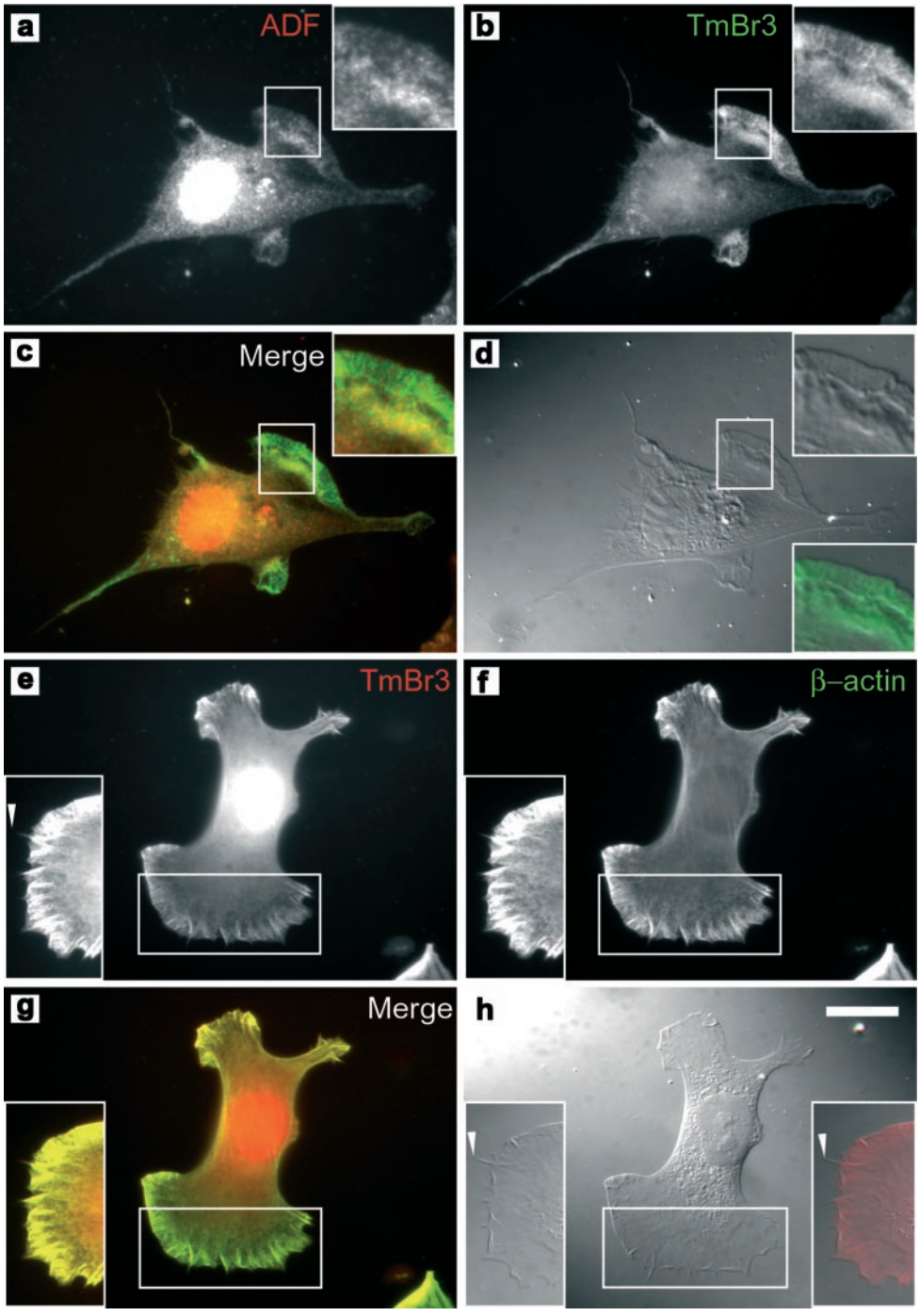

Figure 9. TmBr3 localization extends to the edge of lamellipodia, but not to the tips of microspikes. (a) 5H cells transiently transfected with TmBr3 immunostained with ADF and TmBr3 (b), showing that there is an overlap in staining at the rear of the lamellipodium as seen by the yellow color in c, a merge of a (red) and b (green). (d) DIC image of the corresponding cell. TmBr3 localization extends to the edge of the lamellipodium as shown in the merged image of (d) (red) and (b) (green) in the lower right insert. (e) TmBr3 and β-actin (f) colocalize in the lamellipodium of 5H cells transiently transfected with TmBr3. (g) Merged image of e (red) and f (green). (h) DIC image of the corresponding cell. Insert shows that TmBr3 localization extends to the edge of the lamellipodium but not to the tip of the microspikes (arrowheads, e and h). Scale bar, 10 μm.

Tms Are Associated with Molecularly Distinct Actin Populations

$hTm5_{NM1}$ was able to recruit myosin II into $hTm5_{NM1}$-containing structures in B35 cells, in intact brain and cultured primary neurons from transgenic animals. The increased contractility of stress fibers was supported by the very large increases in MLC phosphorylation in the 5H and 5 M cell lines. In addition, myosin isoform specificity for the $hTm5_{NM1}$-based stress fibers was observed. Distinct functional properties for myosin IIA (Wylie and Chantler, 2001) and B (Bridgman *et al.*, 2001) have been observed, and the ability of Tms to distinguish between these isoforms confers another level of functional specificity to Tm-containing actin filaments. The ability to associate with one type of myosin II isoform was not absolute. In growth cones that have no IIA, IIB was able to colocalize with $hTm5_{NM1}$ in contrast to the

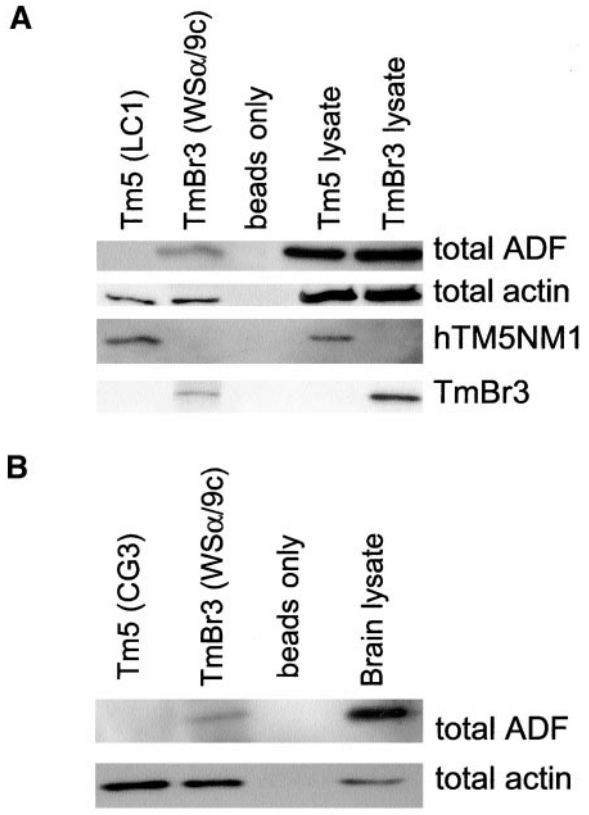

Figure 10. ADF coimmunoprecipitates with TmBr3 but not with $hTm5_{NM1}$. (a) $hTm5_{NM1}$ was immunoprecipitated from the 5H cells using the LC1 antibody. TmBr3 was immunoprecipitated from the Br3H cells with the WSα/9c antibody. ADF was coimmunoprecipitated with TmBr3 but not $hTm5_{NM1}$. Both tropomyosin isoforms were able to coimmunoprecipitate actin. LC1 does not detect TmBr3 and WSα/9c does not detect $hTm5_{NM1}$. (b) ADF was coimmunoprecipitated from whole adult wild-type mouse brain using the WSα/9c antibody. The CG3 antibody that detects $hTm5_{NM1}$ was unable to coimmunoprecipitate ADF. Both WSα/9c and CG3 were able to coimmunoprecipitate actin.

preferential association of IIA in stress fibers. This work together with Fanning *et al.* (1994) suggests that a molecular "hierarchy" may exist where the association of myosins with specific Tm-containing microfilaments may be dependent on the availability or levels of specific myosin isoforms.

Supportive of an increased stability of stress fibers in the 5H cells was a dramatic increase in phosphorylated, inactive ADF. ADF is thought to increase filament turnover and severing when bound. Inactivation by Lim kinase phosphorylation prevents ADF binding to the actin filament (Arber *et al.*, 1998; Yang *et al.*, 1998). ADF and a few Tm isoforms have been shown to compete for binding to actin filaments in vitro (Bernstein and Bamburg, 1982) and in *Caenorhabditis elegans* muscle (Ono and Ono, 2002). Our results strongly suggest that increased Tm5/5a levels were able to actively compete ADF from actin filaments, as inferred from the high levels of inactive PADF in these cells. The balance between Lim kinase and phosphatase may then be reset favoring ADF phosphorylation and further preventing the binding of ADF to filaments. The Tm5/5a stress fibers were therefore myosin rich and ADF depleted.

The results of the TmBr3 experiments were in direct contrast to those of $hTm5_{NM1}$. Br3H and Br3 M cells showed a significant decrease in MLC phosphorylation, which was consistent with the reduction in stress fibers observed. This is suggestive though not conclusive of a lack of engagement of myosin II with small TmBr3 filaments. Myosin II has been observed attached to the small filaments associated with post-golgi vesicles, which are nontension bearing (Heimann *et al.*, 1999).

Our coimmunoprecipitation data showed the association of TmBr3 and not $hTm5_{NM1}$ with ADF-containing actin filaments both in the B35 cells and intact brain. TmBr3 and ADF colocalized in TmBr3-transfected cells, and the staining patterns within the intact cerebellum are very similar (Had *et al.*, 1994; Weinberger *et al.*, 1996). This conflicts with previous reports of the mutually exclusive association of ADF and Tm with actin filaments (Bernstein and Bamburg, 1982; Ono and Ono, 2002). These studies were primarily done in vitro and used a very limited number of Tm isoforms, most of which were the larger HMW Tms, such as those present in muscle, whereas the majority of nonmuscle Tms are LMW (like TmBr3). We have also observed the colocalization of ADF and LMW Tms in growth cones of primary cortical neurons (G. Schevzov *et al.*, in preparation). Clearly, not all Tm isoforms are absent from ADF bound filaments. The studies of Lehman *et al.* (2000) using both LMW and HMW mammalian Tms as well as yeast Tms clearly show the ability of Tm isoforms to bind in different positions along the actin filament. These authors have suggested that this property of Tm isoforms may differentially affect the interaction of other actin-binding proteins. It is possible that the TmBr3-enriched Tm polymer may bind in a position along the actin filaments that does not compete for binding with ADF. The ADF induced twist of the actin helix may, in fact, be the preferred structure for TmBr3 incorporation. The dominance of ADF- and TmBr3-associated actin filaments over stress fibers indicates that these structures have powerful effects on cellular actin dynamics. Neurons possess high levels of TmBr3 and are a cell type that do not possess stress fibers even when cultured (Stamm *et al.*, 1993; Weinberger *et al.*, 1996; Bradke and Dotti, 1999). The presence of TmBr3/ADF filaments may be a method of tailoring actin filament structure appropriate for neuronal cells. In this context TmBr3 is only expressed in neurons after differentiation has begun and TmBr3 can be induced in PC12 cells stimulated to differentiate into a neuronal morphology (Weinberger *et al.*, 1993). However, there are now a number of isoforms that are highly homologous to TmBr3 that are expressed in nonneuronal tissue (Dufour *et al.*, 1998). This certainly raises the possibility that other Tm isoforms will possess similar properties.

ACKNOWLEDGMENTS

We thank Heather Loch, Ornella Tolhurst, Jenny Meaney, Josephine Joya, and Rowena Almonte-Baldonado for technical assistance. We also thank Professor Bob Adelstein for the MHC antibodies. This work was supported by the Australian National Health and Medical Research Council (NHMRC) grants to R.W., P.G., P.J., and E.H., and a U.S. Public Health Service NIH grant GM35126 to J.R.B. N.B. was

supported by a NHMRC Dora Lush Postgraduate Research Scholarship. P.G. is a Principal Research Fellow of the NHMRC.

REFERENCES

Amano, M., Ito, M., Kimura, K., Fukata, Y., Chihara, K., Nakano, T., Matsuura, Y., and Kaibuchi, K. (1996). Phosphorylation and activation of myosin by Rho-associated kinase (Rho-kinase). J. Biol. Chem. *271*, 20246–20249.

Arber, S., Barbayannis, F.A., Hanser, H., Schneider, C., Stanyon, C.A., Bernard, O., and Caroni, P. (1998). Regulation of actin dynamics through phosphorylation of cofilin by LIM-kinase. Nature *393*, 805–809.

Bamburg, J.R. (1999). Proteins of the ADF/cofilin family: essential regulators of actin dynamics. Annu. Rev. Cell Dev. Biol. *15*, 185–230.

Bamburg, J.R., and Bray, D. (1987). Distribution and cellular localization of actin depolymerizing factor. J. Cell Biol. *105*, 2817–2825.

Beisel, K.W., and Kennedy, J.E. (1994). Identification of novel alternatively spliced isoforms of the tropomyosin-encoding gene, TMnm, in the rat cochlea. Gene *143*, 251–256.

Berens, M.E., Rief, M.D., Loo, M.A., and Giese, A. (1994). The role of extracellular matrix in human astrocytoma migration and proliferation studied in a microliter scale assay. Clin. Exp. Metastasis *12*, 405–415.

Bernstein, B.W., and Bamburg, J.R. (1982). Tropomyosin binding to F-actin protects the F-actin from disassembly by brain actin-depolymerizing factor (ADF). Cell Motil. *2*, 1–8.

Bradke, F., and Dotti, C.G. (1999). The role of local actin instability in axon formation. Science *283*, 1931–1934.

Bridgman, P.C., Dave, S., Asnes, C.F., Tullio, A.N., and Adelstein, R.S. (2001). Myosin IIB is required for growth cone motility. J. Neurosci. *21*, 6159–6169.

Chrzanowska-Wodnicka, M., and Burridge, K. (1996). Rho-stimulated contractility drives the formation of stress fibers and focal adhesions. J. Cell Biol. *133*, 1403–1415.

Cooley, B.C., and Bergtrom, G. (2001). Multiple combinations of alternatively spliced exons in rat tropomyosin-alpha gene mRNA: evidence for 20 new isoforms in adult tissues and cultured cells. Arch. Biochem. Biophys. *390*, 71–77.

Drees, B., Brown, C., Barrell, B.G., and Bretscher, A. (1995). Tropomyosin is essential in yeast, yet the TPM1 and TPM2 products perform distinct functions. J. Cell Biol. *128*, 383–392.

Dufour, C., Weinberger, R.P., Schevzov, G., Jeffrey, P.L., and Gunning, P. (1998). Splicing of two internal and four carboxyl-terminal alternative exons in nonmuscle tropomyosin 5 pre-mRNA is independently regulated during development. J. Biol. Chem. *273*, 18547–18555.

Fanning, A.S., Wolenski, J.S., Mooseker, M.S., and Izant, J.G. (1994). Differential regulation of skeletal muscle myosin-II and brush border myosin-I enzymology and mechanochemistry by bacterially produced tropomyosin isoforms. Cell Motil. Cytoskel. *29*, 29–45.

Gimona, M., Watakabe, A., and Helfman, D.M. (1995). Specificity of dimer formation in tropomyosins: influence of alternatively spliced exons on homodimer and heterodimer assembly. Proc. Natl. Acad. Sci. USA *92*, 9776–9780.

Goodwin, L.O., Lees-Miller, J.P., Leonard, M.A., Cheley, S.B., and Helfman, D.M. (1991). Four fibroblast tropomyosin isoforms are expressed from the rat alpha-tropomyosin gene via alternative RNA splicing and the use of two promoters. J. Biol. Chem. *266*, 8408–8415.

Gunning, P., Hardeman, E., Jeffrey, P., and Weinberger, R. (1998a). Creating intracellular structural domains: spatial segregation of actin and tropomyosin isoforms in neurons. Bioessays *20*, 892–900.

Gunning, P., Weinberger, R., Jeffrey, P., and Hardeman, E. (1998b). Isoform sorting and the creation of intracellular compartments. Annu. Rev. Cell Dev. Biol. *14*, 339–372.

Had, L., Faivre-Sarrailh, C., Legrand, C., Mery, J., Brugidou, J., and Rabie, A. (1994). Tropomyosin isoforms in rat neurons: the different developmental profiles and distributions of TM-4 and TMBr-3 are consistent with different functions. J. Cell Sci. *107*, 2961–2973.

Hannan, A.J., Schevzov, G., Gunning, P., Jeffrey, P.L., and Weinberger, R.P. (1995). Intracellular localization of tropomyosin mRNA and protein is associated with development of neuronal polarity. Mol. Cell. Neurosci. *6*, 397–412.

Heimann, K., Percival, J.M., Weinberger, R., Gunning, P., and Stow, J.L. (1999). Specific isoforms of actin-binding proteins on distinct populations of Golgi-derived vesicles. J. Biol. Chem. *274*, 10743–10750.

Hitchcock-DeGregori, S.E., Sampath, P., and Pollard, T.D. (1988). Tropomyosin inhibits the rate of actin polymerization by stabilizing actin filaments. Biochemistry *27*, 9182–9185.

Hogan, P., Beddington, R., Costantini, F., and Lacy, E. (1994). Manipulating the Embryo. Cold Spring Harbor, NY: Cold Spring Harbor Laboratory Press.

Hughes, J.A.I, Cooke-Yarborough, C.M., Chadwick, N.C., Schevzov, G., Arbuckle, S.M., Gunning P., and Weinberger R.P. High molecular weight tropomyosins localize to the contractile rings of dividing CNS cells but are absent from malignant pediatric and adult CNS tumors. GLIA (*in press*).

Ishikawa, R., Yamashiro, S., and Matsumura, F. (1989). Differential modulation of actin-severing activity of gelsolin by multiple isoforms of cultured rat cell tropomyosin. Potentiation of protective ability of tropomyosins by 83-kDa nonmuscle caldesmon. J. Biol. Chem. *264*, 7490–7497.

Kawano, Y., Fukata, Y., Oshiro, N., Amano, M., Nakamura, T., Ito, M., Matsumura, F., Inagaki, M., and Kaibuchi, K. (1999). Phosphorylation of myosin-binding subunit (MBS) of myosin phosphatase by Rho-kinase in vivo. J. Cell Biol. *147*, 1023–1038.

Kimura, K. *et al.* (1996). Regulation of myosin phosphatase by Rho and Rho-associated kinase (Rho-kinase). Science *273*, 245–248.

Lees-Miller, J.P., Goodwin, L.O., and Helfman, D.M. (1990). Three novel brain tropomyosin isoforms are expressed from the rat alpha-tropomyosin gene through the use of alternative promoters and alternative RNA processing. Mol. Cell. Biol. *10*, 1729–1742.

Lehman, W. *et al.* (2000). Tropomyosin and actin isoforms modulate the localization of tropomyosin strands on actin filaments. J. Mol. Biol. *302*, 593–606.

Lessard, J.L. (1988). Two monoclonal antibodies to actin: one muscle selective and one generally reactive. Cell Motil. Cytoskel. *10*, 349–362.

Lin, J.J., Hegmann, T.E., and Lin, J.L. (1988). Differential localization of tropomyosin isoforms in cultured nonmuscle cells. J. Cell Biol. *107*, 563–572.

Matsumura, F., Ono, S., Yamakita, Y., Totsukawa, G., and Yamashiro, S. (1998). Specific localization of serine 19 phosphorylated myosin II during cell locomotion and mitosis of cultured cells. J. Cell Biol. *140*, 119–129.

Matsumura, F., and Yamashiro-Matsumura, S. (1985). Purification and characterization of multiple isoforms of tropomyosin from rat cultured cells. J. Biol. Chem. *260*, 13851–13859.

McGough, A., Pope, B., Chiu, W., and Weeds, A. (1997). Cofilin changes the twist of F-actin: implications for actin filament dynamics and cellular function. J. Cell Biol. *138*, 771–781.

Meberg, P.J., Ono, S., Minamide, L.S., Takahashi, M., and Bamburg, J.R. (1998). Actin depolymerizing factor and cofilin phosphorylation dynamics: response to signals that regulate neurite extension. Cell Motil. Cytoskel. *39*, 172–190.

Minamide, L.S., Painter, W.B., Schevzov, G., Gunning, P., and Bamburg, J.R. (1997). Differential regulation of actin depolymerizing factor and cofilin in response to alterations in the actin monomer pool. J. Biol. Chem. *272*, 8303–8309.

Miyado, K., Kimura, M., and Taniguchi, S. (1996). Decreased expression of a single tropomyosin isoform, TM5/TM30nm, results in reduction in motility of highly metastatic B16–F10 mouse melanoma cells. Biochem. Biophys. Res. Commun. *225,* 427–435.

Nishida, E., Muneyuki, E., Maekawa, S., Ohta, Y., and Sakai, H. (1985). An actin-depolymerizing protein (destrin) from porcine kidney. Its action on F-actin containing or lacking tropomyosin. Biochemistry *24*, 6624–6630.

Ono, S., and Ono, K. (2002). Tropomyosin inhibits ADF/cofilin-dependent actin filament dynamics. J. Cell Biol. *156*, 1065–1076.

Percival, J.M., Thomas, G., Cock, T.A., Gardiner, E.M., Jeffrey, P.L., Lin, J.J., Weinberger, R.P., and Gunning, P. (2000). Sorting of tropomyosin isoforms in synchronized NIH 3T3 fibroblasts: evidence for distinct microfilament populations. Cell Motil. Cytoskel. *47*, 189–208.

Pittenger, M.F., and Helfman, D.M. (1992). In vitro and in vivo characterization of four fibroblast tropomyosins produced in bacteria: TM-2, TM-3, TM-5a, and TM-5b are co-localized in interphase fibroblasts. J. Cell Biol. *118,* 841–858.

Pittenger, M.F., Kistler, A., and Helfman, D.M. (1995). Alternatively spliced exons of the beta tropomyosin gene exhibit different affinities for F-actin and effects with nonmuscle caldesmon. J. Cell Sci. *108*, 3253–3265.

Prasad, G.L., Fuldner, R.A., and Cooper, H.L. (1993). Expression of transduced tropomyosin 1 cDNA suppresses neoplastic growth of cells transformed by the ras oncogene. Proc. Natl. Acad. Sci. USA *90*, 7039–7043.

Qin, H., and Gunning, P. (1997). The 3′-end of the human beta-actin gene enhances activity of the beta-actin expression vector system: construction of improved vectors. J. Biochem. Biophys. Methods *36*, 63–72.

Ren, X.D., Kiosses, W.B., and Schwartz, M.A. (1999). Regulation of the small GTP-binding protein Rho by cell adhesion and the cytoskeleton. EMBO J. *18*, 578–585.

Ridley, A.J., and Hall, A. (1992). The small GTP-binding protein rho regulates the assembly of focal adhesions and actin stress fibers in response to growth factors. Cell *70*, 389–399.

Ridley, A.J., Paterson, H.F., Johnston, C.L., Diekmann, D., and Hall, A. (1992). The small GTP-binding protein rac regulates growth factor-induced membrane ruffling. Cell *70*, 401–410.

Rochlin, M.W., Itoh, K., Adelstein, R.S., and Bridgman, P.C. (1995). Localization of myosin II A and B isoforms in cultured neurons. J. Cell Sci. *108*, 3661–3670.

Schevzov, G., Gunning, P., Jeffrey, P.L., Temm-Grove, C., Helfman, D.M., Lin, J.J., and Weinberger, R.P. (1997). Tropomyosin localization reveals distinct populations of microfilaments in neurites and growth cones. Mol. Cell. Neurosci. *8*, 439–454.

Schubert, D., Heinemann, S., Carlisle, W., Tarikas, H., Kimes, B., Patrick, J., Steinbach, J.H., Culp, W., and Brandt, B.L. (1974). Clonal cell lines from the rat central nervous system. Nature *249*, 224–227.

Sellers, J.R. (1991). Regulation of cytoplasmic and smooth muscle myosin. Curr. Opin. Cell Biol. *3*, 98–104.

Sellers, J.R., Pato, M.D., and Adelstein, R.S. (1981). Reversible phosphorylation of smooth muscle myosin, heavy meromyosin, and platelet myosin. J. Biol. Chem. *256*, 13137–13142.

Stamm, S., Casper, D., Lees-Miller, J.P., and Helfman, D.M. (1993). Brain-specific tropomyosins TMBr-1 and TMBr-3 have distinct patterns of expression during development and in adult brain. Proc. Natl. Acad. Sci. USA *90*, 9857–9861.

Sung, L.A., Gao, K.M., Yee, L.J., Temm-Grove, C.J., Helfman, D.M., Lin, J.J., and Mehrpouryan, M. (2000). Tropomyosin isoform 5b is expressed in human erythrocytes: implications of tropomodulin-TM5 or tropomodulin-TM5b complexes in the protofilament and hexagonal organization of membrane skeletons. Blood *95*, 1473–1480.

Svitkina, T.M., and Borisy, G.G. (1999). Arp2/3 complex and actin depolymerizing factor/cofilin in dendritic organization and treadmilling of actin filament array in lamellipodia. J. Cell Biol. *145*, 1009–1026.

Tan, J.L., Ravid, S., and Spudich, J.A. (1992). Control of nonmuscle myosins by phosphorylation. Annu. Rev. Biochem. *61*, 721–759.

Temm-Grove, C.J., Guo, W., and Helfman, D.M. (1996). Low molecular weight rat fibroblast tropomyosin 5 (TM-5): cDNA cloning, actin-binding, localization, and coiled-coil interactions. Cell Motil. Cytoskel. *33*, 223–240.

Trybus, K.M. (1991). Regulation of smooth muscle myosin. Cell Motil. Cytoskel. *18*, 81–85.

Warren, K.S., Lin, J.L., McDermott, J.P., and Lin, J.J. (1995). Forced expression of chimeric human fibroblast tropomyosin mutants affects cytokinesis. J. Cell Biol. *129*, 697–708.

Weinberger, R., Schevzov, G., Jeffrey, P., Gordon, K., Hill, M., and Gunning, P. (1996). The molecular composition of neuronal microfilaments is spatially and temporally regulated. J. Neurosci. *16*, 238–252.

Weinberger, R.P., Henke, R.C., Tolhurst, O., Jeffrey, P.L., and Gunning, P. (1993). Induction of neuron-specific tropomyosin mRNAs by nerve growth factor is dependent on morphological differentiation. J. Cell Biol. *120*, 205–215.

Wessel, D., and Flugge, U.I. (1984). A method for the quantitative recovery of protein in dilute solution in the presence of detergents and lipids. Anal. Biochem. *138*, 141–143.

Wylie, S.R., and Chantler, P.D. (2001). Separate but linked functions of conventional myosins modulate adhesion and neurite outgrowth. Nat. Cell Biol. *3*, 88–92.

Yang, N., Higuchi, O., Ohashi, K., Nagata, K., Wada, A., Kangawa, K., Nishida, E., and Mizuno, K. (1998). Cofilin phosphorylation by LIM-kinase 1 and its role in Rac-mediated actin reorganization. Nature *393*, 809–812.